

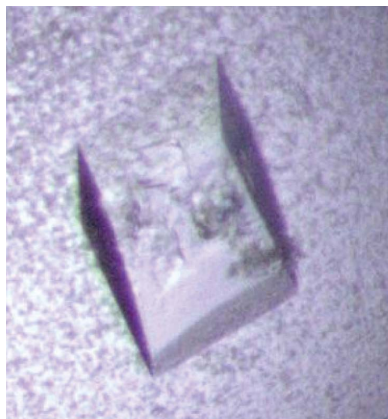
Daisy W. Leung,^a Dominika Borek,^b Mina Farahbakhsh,^{a,c} Parameshwaran Ramanan,^{a,d} Jay C. Nix,^e Tianjiao Wang,^a Kathleen C. Prins,^f Zbyszek Otwinowski,^b Richard B. Honzatko,^a Luke A. Helgeson,^{a,c} Christopher F. Basler^f and Gaya K. Amarasinghe^{a*}

^aDepartment of Biochemistry, Biophysics and Molecular Biology, Iowa State University, Ames, IA 50011, USA, ^bDepartment of Biochemistry, University of Texas Southwestern Medical Center, 5323 Harry Hines Boulevard, Dallas, TX 75390-8816, USA, ^cBiochemistry Undergraduate Program, Iowa State University, Ames, IA 50011, USA, ^dBiochemistry Graduate Program, Iowa State University, Ames, IA 50011, USA, ^eAdvanced Light Source, Lawrence Berkeley National Laboratory, Berkeley, CA 94720, USA, and ^fDepartment of Microbiology, Mount Sinai School of Medicine, New York, NY 10029, USA

Correspondence e-mail: amarasin@iastate.edu

Received 18 December 2009

Accepted 10 April 2010



© 2010 International Union of Crystallography
All rights reserved

Crystallization and preliminary X-ray analysis of Ebola VP35 interferon inhibitory domain mutant proteins

VP35 is one of seven structural proteins encoded by the Ebola viral genome and mediates viral replication, nucleocapsid formation and host immune suppression. The C-terminal interferon inhibitory domain (IID) of VP35 is critical for dsRNA binding and interferon inhibition. The wild-type VP35 IID structure revealed several conserved residues that are important for dsRNA binding and interferon antagonism. Here, the expression, purification and crystallization of recombinant Zaire Ebola VP35 IID mutants R312A, K319A/R322A and K339A in space groups $P6_122$, $P2_12_12_1$ and $P2_1$, respectively, are described. Diffraction data were collected using synchrotron sources at the Advanced Light Source and the Advanced Photon Source.

1. Introduction

Ebola virus (EBOV) is a member of the *Filoviridae* family that causes severe hemorrhagic fever, with human fatality rates as high as 90%. Currently, there are no approved treatments or vaccines to treat EBOV infections (Basler & Amarasinghe, 2009; Bray & Geisbert, 2005; Burton & Parren, 2000). Multifunctional viral protein 35 (VP35) is one of seven structural proteins encoded by the 19 kb EBOV genome and plays a critical role in EBOV pathogenesis, including mediating viral replication, nucleocapsid formation and host immune suppression (Basler & Amarasinghe, 2009). Recent studies have shown that the N-terminal region of VP35 is important for oligomerization, while the C-terminal region is required for dsRNA binding and suppression of host immune responses (Basler *et al.*, 2003; Cardenas *et al.*, 2006; Hartman *et al.*, 2004). We recently solved the crystal structure of the VP35 C-terminal interferon inhibitory domain alone and bound to dsRNA (IID; Leung, Ginder, Fulton *et al.*, 2009; Leung, Ginder, Nix *et al.*, 2009; Leung *et al.*, 2010). Analysis of the VP35 IID structure revealed a central patch of basic residues clustered around a highly conserved Arg312 residue (Fig. 1). Mutation of Arg312 and other residues within this basic patch, including Lys319, Arg322 and Lys339, leads to diminished dsRNA binding and IFN inhibition (Cardenas *et al.*, 2006; Hartman *et al.*, 2004; Leung *et al.*, 2010; Prins *et al.*, 2010). How these basic residues mediate dsRNA binding and facilitate EBOV immune evasion is not known. In order to understand the structural basis of how the mutation of these basic residues leads to a loss of dsRNA binding, we initiated studies to characterize the crystal structures of three VP35 IID mutants: R312A, K319A/R322A and K339A. Here, we describe our efforts to express, purify and crystallize each of these VP35 IID mutant proteins as well as our initial X-ray diffraction data-collection efforts.

2. Methods

2.1. Cloning and expression

PCR products for the VP35 mutants R312A, K319A/R322A and K339A were generated by overlap PCR (Gene ID 911827; Basler *et al.*, 2000) using the coding region for VP35 IID (residues 215–340) from Zaire ebolavirus strain Mayinga as a template. Amplified PCR products were subcloned into a modified pET15b vector (Novagen) which contained a maltose-binding protein (MBP) fusion tag and a

tobacco etch virus protease cleavage site 5' to the multiple cloning site (MCS). Mutations in the resulting vectors were confirmed by sequencing prior to transformation into *Escherichia coli* BL21 (DE3) cells (Novagen). Transformed cells were cultured in LB medium at 310 K to an optical density of 0.6 at 600 nm and were induced with 0.5 mM IPTG overnight at 291 K for protein expression.

2.2. Protein purification

Cells were harvested by centrifugation at 3000g and 277 K for 30 min. Cells were resuspended in lysis buffer consisting of 25 mM sodium phosphate pH 7.0, 1 M NaCl and 5 mM β -mercaptoethanol and stored at 193 K. Each VP35 IID mutant protein was purified as described previously (Leung, Ginder, Nix *et al.*, 2009). Briefly, cells were thawed and lysed using a cell homogenizer (EmulsiFlex-C5, Avestin) prior to centrifugation at 30 000g and 277 K for 30 min. The supernatant was loaded onto a 15 ml amylose column (XK 26/20, GE Healthcare) and eluted with lysis buffer containing 1% maltose. The eluted protein was diluted to a final NaCl concentration of approximately 50 mM with 25 mM sodium phosphate pH 7.0 and 5 mM β -mercaptoethanol and was subsequently loaded onto an 8 ml Source 15S column (packed in a Tricorn 10/100 column, GE Healthcare) using buffer SA (25 mM phosphate pH 7.0, 50 mM NaCl and 5 mM β -mercaptoethanol) and eluted with buffer SB (25 mM phosphate pH 7.0, 1 M NaCl and 5 mM β -mercaptoethanol). The MBP fusion tag was removed by incubation with recombinant tobacco etch virus protease for 3–6 h at 277 K. The cleaved VP35 IID mutant proteins were further purified on Source 15S before a final purification step on a Superdex 75 column (10/300 GL, GE Healthcare) with buffer containing 10 mM HEPES pH 7.0, 150 mM NaCl and 2 mM TCEP.

2.3. ThermoFluor analysis of mutant proteins

The melting temperatures (T_m) of the VP35 IID variants were measured by ThermoFluor assay following established protocols

(Ericsson *et al.*, 2006; Cummings *et al.*, 2006). In brief, experiments were carried out in a MiniOpticon real-time PCR instrument (Bio-Rad). Measurements were performed using an excitation wavelength of 470–505 nm and an emission wavelength of 540–700 nm. Data were acquired using a temperature gradient from 303 to 363 K in 0.5 K increments. The samples contained 20 μ M VP35 IID mutant protein, 1 \times SYPRO Orange (Invitrogen), 10 mM HEPES pH 7, 150 mM NaCl and 2 mM TCEP. The melting curves represent the fluorescence increase arising from the association of SYPRO Orange with exposed hydrophobic residues as the protein unfolds with increasing temperature. Fluorescence data were analyzed and the temperature corresponding to the derivative peak of the curve represents the melting temperature.

2.4. Crystallization

Preliminary crystallization trials for all three mutant VP35 IID proteins were performed using standard commercial screens (Hampton Research) and were further optimized using reagents generated in-house. Native crystals were grown using the hanging-drop vapor-diffusion method at 298 K. Protein solutions in size-exclusion chromatography buffer were diluted in a 1:1 ratio with well solution. Crystals from optimized solutions were initially soaked for 60 s in well solution containing 10% (w/v) glycerol and subsequently soaked for 60 s in well solution containing 25% (w/v) glycerol prior to cryocooling in liquid nitrogen.

2.5. Data collection and processing

Diffraction data for native proteins were collected at the Advanced Light Source (beamline 4.2.2) and at the Advanced Photon Source (beamlines 19-ID and 19-BM) at 100 K on a CCD detector (ADSC Q315 at 19-ID and ADSC Quantum Q210r at 19-BM). For R312A mutant VP35 IID protein, 360 frames were collected at a crystal-to-detector distance of 250 mm using an oscillation range of 0.3°. For K319A/R322A mutant VP35 IID protein, 180 frames were collected at a crystal-to-detector distance of 125 mm using an oscillation range of 1°. For K339A mutant VP35 IID protein, 180 frames were collected at a crystal-to-detector distance of 120 mm using an oscillation range of 1°. Diffraction data were indexed, integrated, scaled and merged using *d*TREK* (Pflugrath, 1999) or *HKL-2000* (Minor *et al.*, 2006). Intensities were converted to structure factors using the *CCP4* program *TRUNCATE* (Collaborative Computational Project, Number 4, 1994; French & Wilson, 1978).

3. Results and discussion

The VP35 IID mutants (R312A, K319A/R322A and K339A) were cloned, expressed and purified to homogeneity as assessed by Coomassie staining of SDS-PAGE gels (Fig. 2a). Analysis of the chromatograms from size-exclusion columns indicated similar elution volumes (12.9 ml for R312A, 12.8 ml for K319A/R322A and 12.6 ml for K339A), suggesting that these proteins retained the hydrodynamic radius of wild-type VP35 IID (Fig. 2a; Leung, Ginder, Nix *et al.*, 2009). However, ThermoFluor analysis revealed that the mutant VP35 IID proteins have different T_m values (Figs. 2b and 2c).

Interestingly, each of the three VP35 IID mutants crystallized under different conditions and belonged to a different space group. Bipyramidal crystals of the VP35 IID R312A mutant protein grew in 1.85 M sodium phosphate/0.15 M potassium phosphate pH 4.15 at a protein concentration of 26 mg ml⁻¹ within 2–3 d to dimensions of 100 μ m in length and about 60 μ m at the thickest area (Fig. 3a). R312A mutant crystals diffracted to 1.95 Å resolution and belonged

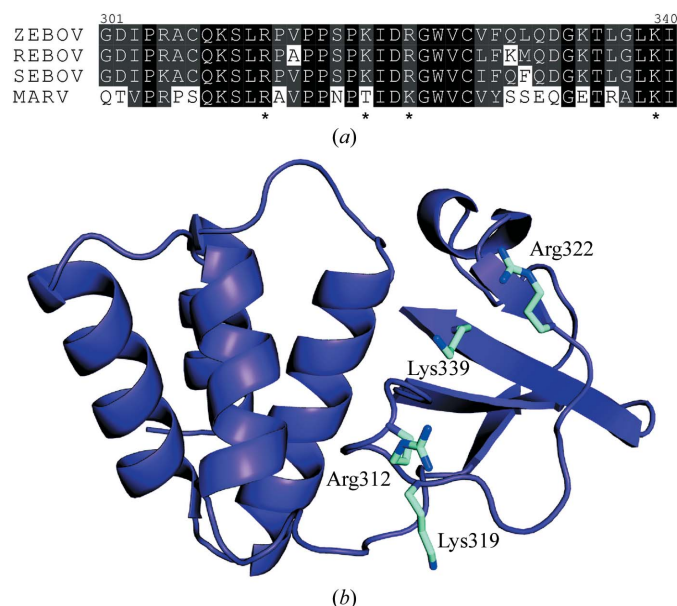
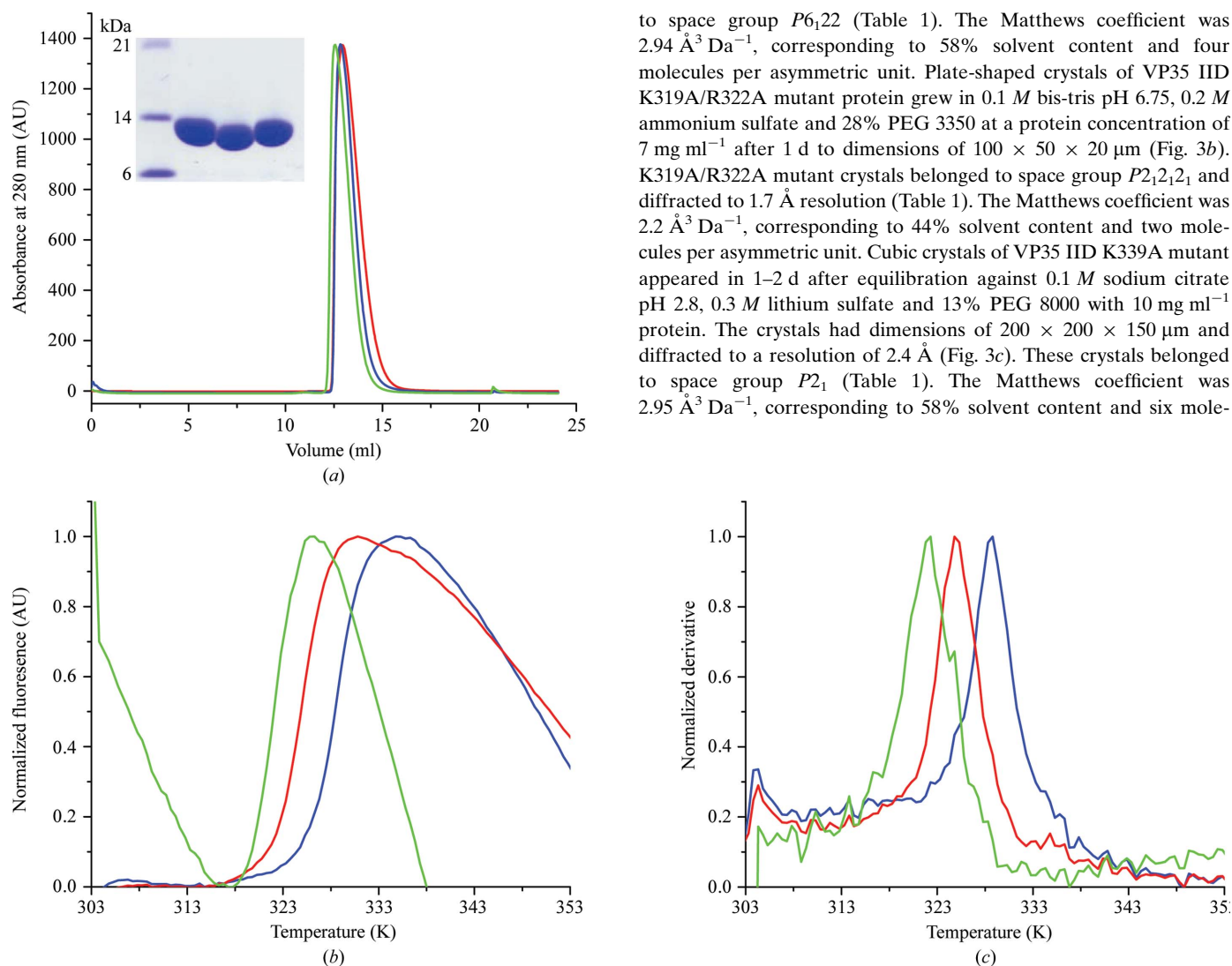
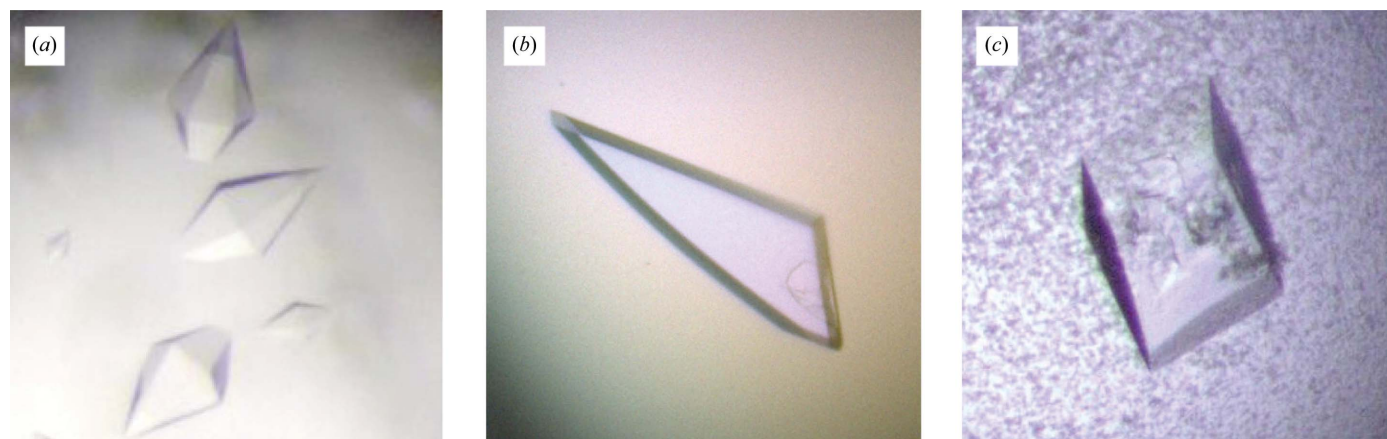


Figure 1
(a) Multiple sequence alignment of VP35 IID residues 301–340 from Ebola virus strains Zaire (ZEBOV), Reston (REBOV) and Sudan (SEBOV) and Marburg virus. The highly conserved basic residues Arg312, Lys319, Arg322 and Lys339 which are important for dsRNA binding are indicated by asterisks. (b) Residues Arg312, Lys319, Arg322 and Lys339 are located in the β -sheet subdomain of VP35 IID.


Figure 2

Biophysical analysis of mutant proteins. (a) Representative chromatograms from analytical size-exclusion columns of VP35 IID mutants R312A (blue), K319A/R322A (red) and K339A (green). The inset shows a Coomassie-stained SDS-PAGE gel of the highly purified final protein samples used in the crystallization trials. Sample order (from left to right) is R312A, K319A/R322A and K339A. (b) Normalized fluorescence emission data for ThermoFluor assays of VP35 IID mutants. Curves are colored as in (a). (c) The derivatives of the data in (b) show differences in T_m values for mutant proteins. The T_m values for R312A, K319A/R322A and K339A are 330 ± 0.2 , 325.3 ± 0.2 and 323.0 ± 0.7 K, respectively. Curves are colored as in (a).


Figure 3

Representative crystals of VP35 IID mutants. (a) R312A (approximate dimensions $30 \times 30 \times 100 \mu\text{m}$), (b) K319A/R322A (approximate dimensions $100 \times 50 \times 20 \mu\text{m}$) and (c) K339A (approximate dimensions $200 \times 200 \times 150 \mu\text{m}$).

Table 1

Data collection for mutant VP35 IID proteins.

Values in parentheses are for the highest resolution shell.

	VP35 IID		
	R312A	K319A/R322A	K339A
Space group	$P6_122$	$P2_12_12_1$	$P2_1$
Unit-cell parameters (Å, °)	$a = b = 81.55,$ $c = 343.50,$ $\alpha = \beta = 90,$ $\gamma = 120$	$a = 51.43, b = 66.07,$ $c = 72.64,$ $\alpha = \beta = \gamma = 90$	$a = 53.39, b = 91.88,$ $c = 102.69,$ $\alpha = \gamma = 90,$ $\beta = 99.60$
Wavelength (Å)	0.979	0.979	0.979
Resolution (Å)	40.49–1.95 (1.97–1.95)	36.32–1.70 (1.76–1.70)	50.00–2.40 (2.44–2.40)
R_{merge}^\dagger (%)	9.2 (n/a)‡	8.9 (58.5)	4.4 (43.3)
Average $I/\sigma(I)$	27.0 (2.3)	9.4 (2.8)	29.0 (2.8)
Completeness (%)	99.6 (100.0)	97.5 (88.3)	99.8 (100.0)
Multiplicity of observation	11.4 (10.7)	6.34 (4.96)	3.8 (3.7)

$^\dagger R_{\text{merge}} = \sum_{hkl} \sum_i |I_i(hkl) - (I(hkl))| / \sum_{hkl} \sum_i I_i(hkl)$, where i runs over multiple observations of the same intensity and hkl runs over all crystallographically unique intensities. ‡ If R_{merge} exceeds 1.0, *SCALEPACK* does not report its value because it is uninformative. Instead, the $I/\sigma(I)$ criterion is used to define resolution cutoff.

cules per asymmetric unit. Data-collection statistics for all three mutant VP35 IID proteins are summarized in Table 1.

All three mutants of VP35 IID displayed diminished dsRNA binding and interferon inhibition without affecting the structural integrity of the protein (Cardenas *et al.*, 2006; Leung *et al.*, 2010; Prins *et al.*, 2010). Interestingly, all four residues that we mutated are surface residues with high degrees of conformational flexibility (Lys and Arg) and their mutation to alanine would result in surface-entropy reduction (Cieslik & Derewenda, 2009; Derewenda & Vekilov, 2006). Identification of these residues for further analysis was primarily based on their sequence conservation and their location within the central basic patch, which we have recently shown to be important for interferon inhibition. Analysis of these mutant structures will provide insight into structural and mechanistic aspects of Ebola VP35-mediated circumvention of the host immune response. Additional analysis of the crystal contacts of these structures will provide correlations between surface conformational entropy and crystal lattice formation. These efforts will be reported shortly.

We thank ISU Biotechnology Facilities and Dr J. Hoy for providing access to instrumentation. We thank L. Tantral, C. Brown and D. Peterson for laboratory assistance and Drs. S. Ginell, N. Duke, F.

Rotella, M. Cuff and J. Lazarz at APS Sector 19. Use of Argonne National Laboratory Structural Biology Center beamlines at the Advanced Photon Source was supported by the US DOE under contract DE-AC02-06CH11357. This work was supported by NIH grants [1F32AI084324 to DWL, R01GM053163 to ZO, R01NS010546 to RBH, R01AI059536 and AI057158 (Northeast Biodefense Center-Lipkin) to CFB and R01AI081914 to GKA], an MRCE Developmental Grant [U54AI057160-Virgin(PI) to GKA] and the Roy J. Carver Charitable Trust (09-3271 to GKA).

References

Basler, C. F. & Amarasinghe, G. K. (2009). *J. Interferon Cytokine Res.* **29**, 511–520.

Basler, C. F., Mikulasova, A., Martinez-Sobrido, L., Paragas, J., Muhlberger, E., Bray, M., Klenk, H. D., Palese, P. & Garcia-Sastre, A. (2003). *J. Virol.* **77**, 7945–7956.

Basler, C. F., Wang, X., Muhlberger, E., Volchkov, V., Paragas, J., Klenk, H. D., Garcia-Sastre, A. & Palese, P. (2000). *Proc. Natl Acad. Sci. USA*, **97**, 12289–12294.

Bray, M. & Geisbert, T. W. (2005). *Int. J. Biochem. Cell Biol.* **37**, 1560–1566.

Burton, D. R. & Parren, P. W. (2000). *Nature (London)*, **408**, 527–528.

Cardenas, W. B., Loo, Y. M., Gale, M. Jr, Hartman, A. L., Kimberlin, C. R., Martinez-Sobrido, L., Saphire, E. O. & Basler, C. F. (2006). *J. Virol.* **80**, 5168–5178.

Cieslik, M. & Derewenda, Z. S. (2009). *Acta Cryst.* **D65**, 500–509.

Collaborative Computational Project, Number 4 (1994). *Acta Cryst.* **D50**, 760–763.

Cummings, M. D., Farnum, M. A. & Nelen, M. I. (2006). *J. Biomol. Screen.* **11**, 854–863.

Derewenda, Z. S. & Vekilov, P. G. (2006). *Acta Cryst.* **D62**, 116–124.

Ericsson, U. B., Hallberg, B. M., Detitta, G. T., Dekker, N. & Nordlund, P. (2006). *Anal. Biochem.* **357**, 289–298.

French, S. & Wilson, K. (1978). *Acta Cryst.* **A34**, 517–525.

Hartman, A. L., Towner, J. S. & Nichol, S. T. (2004). *Virology*, **328**, 177–184.

Leung, D. W., Ginder, N. D., Fulton, D. B., Nix, J., Basler, C. F., Honzatko, R. B. & Amarasinghe, G. K. (2009). *Proc. Natl Acad. Sci. USA*, **106**, 411–416.

Leung, D. W., Ginder, N. D., Nix, J. C., Basler, C. F., Honzatko, R. B. & Amarasinghe, G. K. (2009). *Acta Cryst.* **F65**, 163–165.

Leung, D. W., Prins, K. C., Borek, D. M., Farahbakhsh, M., Tufariello, J. M., Ramanan, P., Nix, J. C., Helgeson, L. A., Otwinowski, Z., Honzatko, R. B., Basler, C. F. & Amarasinghe, G. K. (2010). *Nature Struct. Mol. Biol.* **17**, 165–172.

Minor, W., Cymborowski, M., Otwinowski, Z. & Chruszcz, M. (2006). *Acta Cryst.* **D62**, 859–866.

Pflugrath, J. W. (1999). *Acta Cryst.* **D55**, 1718–1725.

Prins, K. C., Delpeut, S., Leung, D. W., Reynard, O., Volchkova, V. A., Reid, S. P., Ramanan, P., Cardenas, W. B., Amarasinghe, G. K., Volchkov, V. E. & Basler, C. F. (2010). *J. Virol.* **84**, 3004–3015.